

## CHAPTER 4

# AEROSOL SAMPLE ANALYSIS

### 4.1 SAMPLE HANDLING PROCEDURES

The sample handling procedures were specified in a standard operating procedures document prepared prior to the study (Appendix 3).

The field operations were conducted from three field stations: one near the Tahoma Woods site, one near the Marblemount site, and one near the Puyallup site. The primary sites were serviced four times per week at 08:00. The secondary sites were serviced weekly.

The Teflon filters used for gravimetric analysis were preweighed and loaded into cassettes at the University of California at Davis (UCD) and shipped to the field stations in standard shipping containers. This included the filters for modules 1 (fine) and 5 (PM<sub>10</sub>) at the primary sites and all filters for the secondary sites. All filters except PM<sub>10</sub> were also preanalyzed for filter opacity for the absorption measurement. The other filters for the primary sites were loaded into cassettes at the field stations. After collection, the cassettes prepared at UCD were shipped to UCD for unloading. Primary cassettes loaded at the field stations were unloaded at the field stations and stored in Petri dishes. The quartz filters for carbon and SO<sub>2</sub> measurement were stored in refrigerators. One designated field blank was included for every seven normal samples.

The sample handling procedures at the UCD laboratory and at the field stations followed those of the normal Interagency Monitoring of Protected Visual Environments (IMPROVE) network.<sup>1</sup> The identification of each sample by site and collection date was done at the field stations.

The procedures for changing cassettes at each site followed those of the normal IMPROVE network:

1. The ambient temperature was recorded.
2. The final flow rate and elapsed time readings were recorded.
3. The exposed cassettes were removed, sealed and placed in the shipping container.
4. The clean cassettes were installed.
5. The initial flow rate readings were recorded.

The procedures for the weekly change at the secondary sites differed from the normal in one detail. The cassette collecting particles at the time of change was shifted from the seventh to the eighth solenoid. When the sample changing was completed, the collection in this cassette was resumed. The sum of both elapsed times was used as the sample duration. All other exposed cassettes were replaced with clean cassettes.

At Hurricane Ridge, Olympic National Park, the sample changing was performed by personnel supplied by the National Park Service. In this case, the containers of pre-identified cassettes were shipped directly to the site.

The Davis Rotating Unit for Monitoring (DRUM) at two primary sites were changed following the normal procedures. All handling of the strips was performed at UCD.

## **4.2 SAMPLE COLLECTION**

### **4.2.1 Summary of Aerosol Collection**

Nearly all of the aerosol collection was done by fine particle modules at the IMPROVE aerosol monitoring samplers. These modules consisted of an inlet to remove large particles and rain, a cyclone to remove coarse particles, four filter cassettes and solenoids, a critical orifice for flow control, and a pump. The sequencing of the solenoids was performed by a clock timer either inside the module or in a separate module.

At the 31 secondary sites, 24-hour samples were collected on Teflon filters. At the three primary sites, 12-hour fine particle samples were collected on Teflon, quartz, and two nylon filters. One nylon module had a denuder coated with sodium carbonate, while the other had no denuder. In addition, there were 12-hour samples of PM<sub>10</sub> (using a standard commercial inlet) and SO<sub>2</sub> (using an impregnated filter). At Tahoma Woods, 23-hour samples were collected on Teflon for the second half of the study.

Aircraft samples were collected on July 25 and 26, using a Teflon/SO<sub>2</sub> (impregnated) filter pack. The sampler used an 8 μm Nuclepore prefilter to define the 2.1 μm cutpoint for the Teflon filter. There were two samples of general background, two slash burn plumes, two Centralia Power Plant plumes, and one urban plume.

Size-resolved samples were collected at Tahoma Woods using 8-stage and 4-stage DRUM samplers and at Marblemount using a 4-stage sampler. An additional remote site in North Cascades National Park (Hozomeen) had a prototype that collected particles between 0.24 and 2.5 μm on a single drum stage.

The DRUM sampler is a Lundgren-type rotating drum cascade impactor using a series of single round jets for each stage. The orifices decrease in size from the first to last stage, with the final orifice providing flow control at about 1.1 LPM by operating as a critical orifice. Behind the last stage there is a tandem Teflon filter with the second filter as a protective filter. The size ranges for the 8-stage and 4-stage versions are listed in Table 4-1.

Table 4-1. Particle size ranges ( $d_{50}$ ) of 8-stage and 4-stage DRUM samplers.

8-Stage		4-Stage	
1	> 10.0 $\mu\text{m}$	1	> 10.0 $\mu\text{m}$
2	5.0 - 10.0 $\mu\text{m}$	2	2.5 - 10.0 $\mu\text{m}$
3	2.5 - 5.0 $\mu\text{m}$		
4	1.1 - 2.5 $\mu\text{m}$	3	0.34 - 2.5 $\mu\text{m}$
5	0.56 - 1.1 $\mu\text{m}$		
6	0.35 - 0.56 $\mu\text{m}$		
7	0.24 - 0.34 $\mu\text{m}$	4	0.069 - 0.34 $\mu\text{m}$
8	0.069 - 0.24 $\mu\text{m}$		
after	< 0.069 $\mu\text{m}$	after	< 0.069 $\mu\text{m}$

The particles were collected on greased-mylar strips on slowly rotating cylindrical drums. The 8-stage version had a rotation rate of 2 mm every 12 hours, while the 4-stage version rotated at 2 mm every 4 hours. (The analytical system was designed to analyze 2 mm segments.)

The problem of bounce-off is minimized during collection by three factors: (1) environmental aerosols tend to be hygroscopic and stick upon contact with surfaces; (2) the mylar is coated with an oily film to prevent bounce; and (3) the rotation prevents excessive build-up of deposited material by spreading the deposit along a 16.8 cm trace.

#### 4.2.2 Period of Record and Sample Recovery

The sample collection began on June 5 at Tahoma Woods, on June 8 at Marblemount, and on June 15 (the planned start date) at most secondary sites. The elemental analysis for the secondary sites was begun with samples collected on June 21. Three sites started late because of heavy snow: Mount Baker (June 25), Sobieski Mountain (July 16), and Paradise (July 20). The southernmost site, Sauvie Island, did not begin until July 18, because of difficulties in obtaining a suitable location.

Several secondary sites had pump failures during the initial week because of faulty design of the rainshields. These were modified and the pumps replaced. For this reason, we began the elemental analysis for the secondary sites on June 21.

Table 4-2 summarizes the period of record and sample recovery rate for each site. The sample recovery rate is the percent of valid samples relative to the possible number of periods from the start date to the end date for that site. For example, Sobieski Mountain had 100% recovery although only 50 samples were collected. In the case of the primary sites, this is based only on the module 1 fine Teflon samples.

Table 4-2. Percent of valid samples in database, based on Teflon filters with PIXE analysis and possible samples from initial to final.

Site	Initial	Final	Valid	Reasons for Loss
<b>PRIMARY</b>				
Tahoma Woods 12h	06/05/90	09/04/90	177 96%	
Tahoma Woods 24h	08/01/90	09/01/90	31 97%	
Marblemount 12h	06/08/90	09/04/90	174 98%	
Paradise 12h	07/20/90	09/04/90	84 89%	electrical short
<b>SECONDARY</b>				
Arlington	06/21/90	09/03/90	74 99%	
Carbon River	06/21/90	09/03/90	75 100%	
Carnation	06/24/90	09/03/90	71 99%	
Carson	06/21/90	09/02/90	72 97%	
Cowlitz	06/21/90	09/03/90	74 99%	
Crystal Mountain	06/21/90	09/03/90	74 99%	
Glenoma	06/21/90	09/03/90	74 99%	
Humtulpis	06/22/90	09/03/90	72 97%	
Hurricane Ridge	06/21/90	08/31/90	69 96%	
Kendall	06/21/90	09/03/90	75 100%	
Kent	06/21/90	09/03/90	68 91%	power surge
La Grande	06/21/90	09/03/90	74 99%	
Mount Baker	06/25/90	09/03/90	65 92%	clock malfunction
Mud Mountain	06/21/90	09/03/90	67 89%	clock malfunction
Newhalem	06/21/90	09/03/90	73 97%	
Nisqually	06/21/90	08/29/90	70 100%	
North Bend	06/21/90	09/02/90	73 99%	
Ohanapacosh	06/21/90	09/03/90	73 97%	
Packwood	06/21/90	09/03/90	66 88%	power outage
Puyallup	06/21/90	09/03/90	73 97%	
Rochester	06/21/90	08/29/90	70 100%	
Sauvie Island	07/18/90	09/02/90	43 91%	schedule problems
Sedro Woolley	06/21/90	09/03/90	70 93%	clogged orifice
Skookumchuck	06/21/90	08/29/90	67 96%	
Sobieski Mountain	07/16/90	09/03/90	50 100%	
South Mountain	06/21/90	09/03/90	73 97%	
Stampede Pass	06/21/90	09/02/90	73 99%	
Sultan	06/21/90	09/03/90	74 99%	
Toutle	06/21/90	09/03/90	65 87%	power outages
Trout Lake	06/21/90	09/02/90	73 99%	
Willapa	06/21/90	09/03/90	73 97%	
<b>TOTAL</b>			2629 96%	

For the entire study, the recovery rate was 96%, indicating that there were no major problems in sample collection. There were three possible reasons. First, all of the samplers had been pretested the previous winter. Second, the field crew were enthusiastic and dedicated. Third, there were no extremes in weather conditions.

Table 4-2 also lists the major reasons for sample loss. The largest single cause was problems in line power, either an outage or a surge. There were a few failures in the electronic circuitry, generally in the clock controllers. Past experience indicates that these types of failures are often associated with power surges. Four samples were lost because of an extremely rare phenomenon, when debris clogged the critical orifice.

Only a small fraction of the DRUM strips have been analyzed, all at Tahoma Woods. This included four weeks for the 4-stage sampler and six weeks for stages 4 through 8 of the 8-stage sampler.

### **4.2.3 Flow Rate**

The flow rate is maintained by a critical orifice located between the filter and pump. The flow rate depends on the diameter of the orifice, and to a smaller degree on the absolute temperature and the pressure drop across the filter. The diameter was adjusted at the beginning of the study for a typical filter and temperature to give the desired flow rate near 22.7 LPM. Once adjusted, the diameter cannot change.

The flow rate is measured before and after collection by two methods. The primary method uses the cyclone as a measuring orifice: the flow rate is a well-defined function of the measured pressure drop across the cyclone. The equation depends on the square root of the absolute temperature and pressure of the air. The secondary method is based on the gauge pressure at the front of the critical orifice and the standard equation of flow through a critical orifice. In both cases, the equations were calibrated using an external measuring orifice. This calibration device was itself calibrated at UCD with a positive-displacement spirometer.

To achieve a 50% capture efficiency in the IMPROVE cyclone, the flow rate should be 22.7 LPM. A flow rate of 20 LPM will result in a 3.5  $\mu\text{m}$  cutpoint, while a flow rate of 25 LPM will result in a 2.0  $\mu\text{m}$  cutpoint.

At the secondary sites, the flow rates were generally slightly higher than 22.7 LPM. The average flow rate ranged from 22.7 to 24.2 LPM. The average 50% cutpoint ranged from 2.2 to 2.5  $\mu\text{m}$ . At a given site the fluctuation was small, with a typical standard deviation of 1%.

At the primary sites, the flow rates through the fine Teflon filters were between 22.2 and 22.8 LPM. The cutpoints were 2.5  $\mu\text{m}$  at Marblemount, 2.6  $\mu\text{m}$  at Paradise, and 2.7  $\mu\text{m}$  at Tahoma Woods. The fluctuations were larger than at the secondary sites because the collection area was reduced by a factor of two; the standard deviations were all 3%.

These variations from 2.5  $\mu\text{m}$  should have a minimal effect on the concentrations. The particles having the largest effect on visibility are predominantly smaller than 2.5  $\mu\text{m}$ .

### 4.3 SAMPLE ANALYSIS

#### 4.3.1 Summary of Sample Analysis

The analysis of the filters collected at the primary sites are summarized in Table 4.3. The analysis of the filters at the secondary sites and the 24-hour filter at Tahoma Woods is the same as for filter 1.

The fine Teflon filters at Tahoma Woods and Paradise and the aircraft samples were also analyzed using the UCD XRF system and the UCD-Stanford synchrotron radiation XRF system.

Table 4-3. Analytical methods applied to the filters collected at primary sites.

Filter	Substrate	Size	Denuder	Analytical Methods
1	Teflon	0 - 2.5 $\mu\text{m}$	none	mass, absorption, PIXE/PESA
2	nylon	0 - 2.5 $\mu\text{m}$	none	ion chromatography
3	nylon	0 - 2.5 $\mu\text{m}$	$\text{Na}_2\text{CO}_3$	ion chromatography
4a	Teflon	0 - 2.5 $\mu\text{m}$	none	
4b	impregnated quartz	gas	-----	ion chromatography
5	Teflon	0 - 10 $\mu\text{m}$	none	mass
6	quartz	0 - 25 $\mu\text{m}$	none	TOR carbon combustion

#### 4.3.2 Gravimetric Analysis

The mass concentration of the fine particles collected on Teflon filters was determined using filter 1 at the primary sites and the only filter at the secondary sites. The  $\text{PM}_{10}$  mass concentration at the primary sites was determined using filter 5. The mass loading on the aircraft samples was insufficient to obtain reliable concentrations.

The procedures followed those of the IMPROVE network. All analyses were performed on a Cahn electromicrobalance. The clean filters were weighed at UCD before being loaded into the sampling cassettes. The exposed filters were weighed on the same balance. The difference was used in calculating the concentration.

The balance was calibrated twice each day and a control filter analyzed. The same filter was analyzed both times each day. The data was examined in two ways. First, the difference between the morning and evening measurements was monitored. For the PREVENT period, the mean of these "reweighs" was  $-0.3 \pm 1.6 \mu\text{m}$ . Second, the average of the two measurements for a

given day was compared to the average determined one month earlier. The difference monitored any gain while in a cassette and any long-term changes in the system. The mean "control" for the PREVENT period was  $0.5 \pm 2.5 \mu\text{m}$ .

### **4.3.3 Absorption Analysis**

The coefficient of absorption is measured on the fine filters used for gravimetric analysis using the UCD Laser Integrating Plate Method (LIPM). Light of wavelength 633 nm from a He(Ne) laser is diffused and collimated to provide a uniform beam of less than  $1 \text{ cm}^2$  at the sample. The light transmitted through the sample is collected with an ORIEL photodiode detection system. The blank Teflon filter does not absorb light but does decrease the transmitted light by scattering. Since this varies from filter to filter, it is necessary to determine the intensity of transmitted light for every clean filter before collection. The intensity of transmitted light for the exposed filters is decreased the same amount by the filter plus any absorption by the particles.

An assumption in the derivation is that there is negligible large-angle scattering from the particles in the sample. This assumption is tested by comparing the LIPM measurements to those determined by an integrating sphere system. The integrating sphere system measures both transmittance and reflectance, thus separating absorption from large angle scattering. The results show that the scattering effect is small, causing an increase in the absorption measurement of approximately 3%. This 3% correction is included in the reported data for the coefficient of absorption.

The integrating plate and integrating sphere measure the absorption by the particles on the filter. Unfortunately, this may differ from the absorption by the particles in the atmosphere. In the atmosphere, the light wave reforms after interacting with a particle, so the absorption by a given particle does not depend on the concentration of other particles. The situation is different for particles on a filter whenever the areal density is high enough to produce overlapping of the particles. The absorbing particle might be shielded from the incident light by other scattering and absorbing particles. The effect will increase with the areal density of particles. A correction equation was determined in a series of tests measuring the same ambient conditions on filters with different areal densities. The correction term increased the average calculated coefficient of absorption by a factor of 2.2.

### **4.3.4 Proton Elemental Analysis (PIXE/PESA)**

The concentrations of elements from Na to Pb on the fine Teflon filters were measured using the UCD Particle Induced X-ray Emission (PIXE) system. A 4.5 MeV proton beam induced the atoms in the sample to emit characteristic x-rays, which were measured by an energy-dispersive Si(Li) detector system. By counting the x-rays at the characteristic energy, the concentration of each element was determined. The system was calibrated using a series of 60 elemental standards.

The x-ray spectrum includes background x-rays in addition to the characteristic x-rays. The spectral analysis program calculates and removes this background, first using a clean Teflon filter and then determining any residual background by smoothing. This background is important in determining the minimum detectable limit (mdl) of an element. A peak can be reliably determined

only if the number of characteristic x-rays exceeds three times the square root of the number of background counts under the peak. This mdl is calculated for every element on each sample. The characteristic peaks are then determined by a peak-searching routine. Finally, the position of the peaks and the number of x-rays is determined by fitting the spectrum to a series of gaussian peaks.

In order to maximize the sensitivity for both light and heavy elements, the UCD PIXE system uses two detectors. The first detector is used for elements Na to Mn, while the second is used for elements Fe to Pb. The two measurements of Fe are monitored by the analysis technician. The second detector is larger, closer to the sample, and has a thicker filter to remove low energy x-rays.

The minimum detection limits in  $\text{ng/m}^3$ , for 12-hour primary and 24-hour secondary Teflon filters are given in Table 4-4. Because the 12-hour filters had one-half of the collection area, the mdl's for both cases were equal. Sulfur was measured above the mdl on every sample. The same was true for most soil elements (Si, K, Ca, Fe, Ti, Mn). Al was occasionally not observed because it is a shoulder on the Si peak. The breakdown by site of the detection of other elements is given in Table 4-5.

Table 4-4. PIXE/PESA minimum detectable limits, in  $\text{ng/m}^3$ , for 12-hr primary and 24-hr secondary samples. The values in parentheses are the percentage of cases the element was detected.

H	1.59 (100%)	Ti	0.58 (95%)	Zn	0.23 (100%)
Al	2.32 (77%)	V	0.49 (76%)	Se	0.25 (12%)
Si	1.65 (100%)	Mn	0.37 (93%)	Br	0.26 (98%)
S	1.45 (100%)	Fe	0.38 (100%)	Sr	0.44 (27%)
K	0.88 (100%)	Ni	0.26 (26%)	Zr	0.65 (13%)
Ca	0.64 (100%)	Cu	0.26 (86%)	Pb	0.60 (94%)

The DRUM strips were analyzed using a single-detector PIXE system. In this case, the beam was collimated to a 2 mm width. The strips were analyzed in 2 mm segments.

The concentration of hydrogen is measured on the Teflon filters concurrently with the PIXE analysis using Proton Elastic Scattering Analysis (PESA). A solid state detector at  $30^\circ$  separates the proton scattered from the hydrogen in the sample from all other protons. By counting the protons at this energy, after subtracting the background, the areal density of hydrogen can be obtained. The system is calibrated using a series of calibrated mylar foils. Because Teflon does not contain hydrogen, the measured protons are from the particles on the filter. The mdl is calculated the same way as with PIXE. Every concentration was above the mdl.

Table 4-5. Percentage of cases when the concentration of a minor element exceeded the PIXE minimum detectable limit.

Site	Zn	Pb	Br	Se	Cu	Cr	Ni	V	As	Na
Tahoma Woods 12h	99	95	95	15	79	56	21	50	53	86
Tahoma Woods 24h	100	100	100	38	97	24	15	59	29	71
Marblemount 12h	99	98	98	13	79	49	26	57	63	74
Paradise 12h	100	87	83	13	56	52	11	36	30	73
Arlington	100	99	100	19	91	3	41	92	58	91
Carbon River	100	93	99	8	91	7	27	73	25	88
Carnation	100	100	100	6	96	6	45	92	66	97
Carson	100	93	100	4	93	11	13	69	21	88
Cowlitz	100	96	99	8	89	15	31	76	18	99
Crystal Mountain	100	93	96	5	77	12	12	65	20	81
Glenoma	100	96	100	11	91	14	12	73	8	92
Humptulips	100	74	97	22	75	13	36	88	8	100
Hurricane Ridge	99	77	96	9	86	10	30	77	3	91
Kendall	100	97	100	15	92	4	29	87	40	89
Kent	100	100	100	18	99	3	35	93	22	90
La Grande	100	96	98	16	82	11	22	80	23	98
Mount Baker	100	94	98	8	91	11	17	66	9	82
Mud Mountain	100	94	100	12	90	12	25	69	30	93
Newhalem	100	92	99	14	90	11	36	88	26	82
Nisqually	100	99	100	6	91	6	27	84	37	99
North Bend	100	100	100	16	93	12	16	88	47	86
Ohanapacosh	100	93	97	8	86	15	15	64	26	89
Packwood	100	95	98	8	88	18	15	64	17	80
Puyallup	100	100	100	8	95	5	68	90	23	100
Rochester	100	91	100	7	79	9	31	77	23	97
Sauvie Island	100	98	100	21	100	7	40	98	14	100
Sedro Woolley	100	100	100	18	93	4	45	99	20	92
Skookumchuck	100	94	99	16	75	0	42	64	7	93
Sobieski Mountain	98	94	94	4	84	12	10	76	14	80
South Mountain	100	84	97	7	86	5	22	75	7	93
Stampede Pass	100	97	92	4	79	8	16	71	19	73
Sultan	100	99	100	11	95	7	1	93	53	78
Toutle	100	92	97	23	82	6	40	82	17	98
Trout Lake	100	95	99	5	70	4	5	44	11	73
Willapa	99	82	96	19	70	7	28	77	9	96
Average	100	94	98	14	86	14	28	76	26	89

At the beginning and end of each analysis session the calibration of the PIXE and PESA systems was checked using a series of calibration standards. A tray of filters analyzed during a normal IMPROVE session was reanalyzed at both times. The PREVENT samples were analyzed in two sessions. For both sessions the correlation for sulfur between the PREVENT and IMPROVE sessions was  $R^2 = 0.998$ . The calculated precision was 3% and the slope differed from 1.0 by less than the standard error of 2%. For hydrogen, the slope was also within 2% of 1.0, but the precision was 10%.

#### 4.3.5 Carbon Analysis

The quartz filters at the primary sites were analyzed at Desert Research Institute (DRI) using the thermal optical reflectance (TOR) method of carbon combustion analysis. A 0.5 cm<sup>2</sup> punch is removed from the sample and loaded into the DRI/OGC analyzer. The sample is heated in a series of six steps to 120°C, 250°C, 450°C, 550°C, 700°C, and 800°C. The sample is kept in a He atmosphere until halfway through the 550°C step. For the remainder of the analysis there is a He/O<sub>2</sub> atmosphere. The reflectance of the sample is monitored with a laser system. The evolved CO<sub>2</sub> is measured by a flame ionization detector (FID). The following steps occur in the 33-minute cycle:

1. The system is purged in He for 120 sec.
2. The sample is injected and the temperature raised to 120°C for 180 sec. The peak (OC1) in the FID is recorded.
3. The temperature is raised to 250°C for 200 sec. The second peak (OC2) is recorded. The reflectance will decrease.
4. The temperature is raised to 450°C for 200 sec. The third peak (OC3) is recorded.
5. The temperature is raised to 550°C and a fourth peak (OC4) is recorded.
6. A He/O<sub>2</sub> atmosphere is introduced while remaining at 550°C. This produces a fifth peak in the FID, produced by pyrolyzed organic carbon. The reflectance also rises; when this value reaches the initial value it is assumed that pyrolyzation is over. All FID counts from this point are counted as the first EC peak (EC1). The total time at 550°C is approximately 600 sec.
7. The temperature is raised to 700°C for 190 sec. The sixth peak (EC2) is recorded.
8. The temperature is raised to 800°C for 100 sec. The seventh peak (EC3) is recorded.
9. CH<sub>4</sub> is injected as a system calibration and the temperature reduced to ambient.

The data is incorporated into the database in four variables:

OCLT	OC1; below 120°C
OCHT	OC2 + OC3 + OC4 + pyrolyzed; 120°C to 550°C
ECLT	EC1; 550°C to 700°C
ECHT	EC2 + EC3; above 700°C

Replicate analyses are obtained by analyzing a second punch.

#### **4.3.6 Ion Analysis (Nylon Filters)**

The concentrations of nitrate, sulfate, nitrite, and chloride ions were measured at Global GeoChemistry (GGC) on the nylon filters collected at the primary sites in modules 2 and 3. The procedures for the ion chromatography analyses are the same as those for the IMPROVE network.

The material on the filters was desorbed in aqueous solution with sodium carbonate. The solution was analyzed by ion chromatography. The system was calibrated after every 25 samples using American Chemical Society (ACS) reagent grade materials. A quality assurance check was made using Environmental Protection Agency (EPA) reference standards. The aqueous solution was monitored for purity. Replicate analyses were periodically performed on the solution.

#### **4.3.7 SO<sub>2</sub> Analysis**

Impregnated quartz filters were prepared by Research Triangle Institute following the procedures used in the IMPROVE network. They analyzed the exposed filters using ion chromatography.

#### **4.3.8 XRF Analysis**

The Teflon filters collected at Tahoma Woods and Paradise were analyzed by two XRF systems: the UCD XRF system and the UCD/Stanford SRXRF system using the cyclotron radiation facility at the Stanford Linear Accelerator. Both systems were calibrated using a series of calibration standards.

The purpose of the XRF analysis was to increase the sensitivity for selenium and other trace elements in this region. Table 4-6 compares the XRF mdl's with the PIXE mdl's. The mdl for the 12-hour Se measurements were 0.24 ng/m<sup>3</sup> for PIXE, 0.05 ng/m<sup>3</sup> for XRF, and 0.04 ng/m<sup>3</sup> for SRXRF. The most important statistic was the fraction of cases in which selenium was measured above the mdl. For the 12-hour samples, Se was above the mdl for 15% of the samples with PIXE, 89% with UCD XRF, and 75% with SRXRF. For the 24-hour samples, the fractions were 43% with PIXE, 100% with UCD XRF, and 77% with SRXRF.

Table 4-6. Minimum detectable limits in ng/m<sup>3</sup> and percentage of cases detected at Tahoma Woods for 12 and 24-hour samples by PIXE, XRF, and SRXRF.

Element	12-HR PIXE	24-HR PIXE	12-HR XRF	24-HR XRF	12-HR SRXRF	24-HR SRXRF
Si	1.61 ( 97%)	1.33 ( 97%)				
S	1.43 (100%)	1.17 (100%)				
K	0.85 (100%)	0.69 (100%)				
Ca	0.62 (100%)	0.50 (100%)				
Ti	0.56 ( 91%)	0.45 ( 82%)				
V	0.48 ( 50%)	0.38 ( 59%)	0.33 ( 64%)	0.19 ( 57%)	0.20 ( 75%)	0.10 ( 94%)
Mn	0.36 ( 94%)	0.28 ( 97%)	0.16 ( 89%)	0.10 (100%)	0.12 (100%)	0.06 (100%)
Fe	0.36 (100%)	0.29 (100%)	0.14 (100%)	0.09 (100%)	0.20 (100%)	0.09 ( 94%)
Ni	0.26 ( 21%)	0.20 ( 15%)	0.08 ( 61%)	0.05 ( 90%)	0.06 ( 88%)	0.03 (100%)
Cu	0.25 ( 79%)	0.20 ( 97%)	0.07 ( 98%)	0.05 ( 97%)	0.05 (100%)	0.03 (100%)
Zn	0.22 ( 99%)	0.18 (100%)	0.07 (100%)	0.04 (100%)	0.04 (100%)	0.02 (100%)
Se	0.24 ( 15%)	0.18 ( 38%)	0.05 ( 89%)	0.03 (100%)	0.04 ( 75%)	0.02 ( 77%)
Br	0.25 ( 95%)	0.19 (100%)	0.06 (100%)	0.04 (100%)	0.05 (100%)	0.02 (100%)
Sr	0.42 ( 27%)	0.31 ( 24%)	0.14 ( 46%)	0.07 ( 63%)		
Zr	0.64 ( 3%)	0.47 ( 6%)				
Pb	0.58 ( 92%)	0.45 (100%)	0.07 ( 98%)	0.04 (100%)	0.07 (100%)	0.03 (100%)

## 4.4 DATA PROCESSING

### 4.4.1 Equations

The flow rates are determined using the pressure drop across the cyclone measured by the magnehelic. The equation is:

$$Q = \sqrt{\frac{T}{293}} a \Delta p^b \quad (4-1)$$

where  $a$  and  $b$  are calibration constraints for each module normalized to 20°C. The temperature was measured at each change.

A second measurement of the flow rate is made using the gauge pressure at the front of the critical orifice. The equation is

$$Q = \sqrt{\frac{T}{293}}(c + d\Delta P) \quad (4-2)$$

where  $c$  and  $d$  are calibration constants for each module normalized to 20°C.

The volume is determined by multiplying the average of the initial and final flow measurements by Equation (4-1) with the duration measured by elapsed time indicators.

The concentrations for mass, carbon, and ions are calculated using

$$C = \frac{m - B}{V} \quad (4-3)$$

where  $m$  is the measured value and  $B$  the artifact, both in  $\mu\text{g}/\text{filter}$ , and  $V$  is the volume in  $\text{m}^3$ . The precision in the concentration will depend on the standard deviation of the field blanks or secondary filters ( $\sigma_{fb}$ ); the fractional precision of the analysis, generally associated with calibration ( $f_{cal}$ ); and the fractional precision in volume ( $f_v$ ). The equation is

$$\sigma^2(C) = \left(\frac{\sigma_{fb}}{V}\right)^2 + 2\frac{Bf_{cal}^2}{V}C + (f_{cal}^2 + f_v^2)C^2. \quad (4-4)$$

For gravimetric analysis,  $f_{cal}^2$  is zero.

The minimum detectable limit (mdl) for these methods is defined to be the concentration at which the precision is 50%. For low concentrations, the first term in Equation (4-4) is much larger than the others. The minimum detectable limit reduces to the form

$$mdl = 2\frac{\sigma_{fb}}{V}. \quad (4-5)$$

Retaining the extra terms would change the numerical value by less than 1% of the value.

The concentration for  $\text{SO}_2$  is calculated using Equation (4-3), except it is multiplied by 2/3 to shift from the measured  $\text{SO}_4$  ion to the calculated  $\text{SO}_2$ .

The equations for PIXE, PESA, and XRF differ from those above for two reasons. First, the analytical methods measure areal density ( $\rho t$ ) in  $\text{ng}/\text{cm}^2$ , so that the collection area enters into the equation for mass per filter of each element. Second, the methodology of using a blank filter to estimate spectral background eliminates the need for subtracting an artifact for any variable. The concentrations are calculated using

$$C = \left(\frac{A}{V}\right)\rho t \quad (4-6)$$

where  $A$  is the area of collection in  $\text{cm}^2$ . The precision includes the statistical precision determined from the number of counts in the peak and background ( $f_s$ ) based on standard Poisson statistics. The equation is

$$\sigma^2(C) = (f_s^2 + f_{cal}^2 + f_v^2)C^2. \quad (4-7)$$

The mdl is defined as the concentration corresponding to a peak with area equal to 3.29 times the square root of the number of background counts under the peak.

The equation for the coefficient of absorption in  $10^{-8} \text{ M}^{-1}$  is

$$b = \left(\frac{A}{V}\right)10^4 \ln\left(\frac{PRE}{POST}\right) \frac{0.97}{R} \quad (4-8)$$

where  $PRE$  and  $POST$  are the two transmission intensities, 0.97 corrects for large angle scattering, and  $R$  is the shielding factor. This shielding factor is expressed in terms of the areal density from gravimetric analysis ( $m$ ) in  $\mu\text{g}/\text{cm}^2$ , using the equation

$$R = 0.36 e^{-m/22} + 0.64 e^{-m/415}. \quad (4-9)$$

The coefficients of this equation are obtained by comparison of collected samples with differing areal densities. The precision is given by

$$\sigma^2(b) = \left(\frac{A}{V} 20 \frac{0.97}{R}\right)^2 \left(\frac{1}{PRE^2} + \frac{1}{POST^2}\right) + \left(0.10 \frac{1-R}{R} b\right) + (f_v b)^2. \quad (4-10)$$

Several composite variables are used in this report. The precision of each composite is determined by simple propagation of uncertainties, using the analytical precision provided with each concentration.

**Sulfur:** The sulfur is assumed to be present as ammonium sulfate. The total sulfate concentration is estimated by multiplying the sulfur from PIXE by 4.125.

**Soil plus K:** The soil component consists of the sum of the predominantly soil elements measured by PIXE, plus oxygen for the normal oxides ( $\text{Al}_2\text{O}_3$ ,  $\text{SiO}_2$ ,  $\text{CaO}$ ,  $\text{K}_2\text{O}$ ,  $\text{FeO}$ ,  $\text{Fe}_2\text{O}_3$ ,  $\text{TiO}_2$ ), plus a factor for unmeasured compounds. Potassium is treated separately because fine potassium can be derived from both soil and smoke. Studies of coarse particles throughout the United States indicated that the K/Fe ratio for soil is approximately 0.6, equal to the value for sediment. Thus, K is eliminated from the calculation and the Fe value is measured to compensate. As discussed below, the excess (nonsoil) potassium is calculated separately. In calculating reconstructed mass, both are included so that 0.6 factor has no effect. The equation for fine soil is:

$$SOIL = 2.20xAl + 2.494xSi + 1.63xCa + 2.42xFe + 1.94xTi. \quad (4-11)$$

If an element is below the mdl, the concentration and precision are both assumed to be equal to mdl/2. The soil variable is always positive. Potassium is not explicitly included because it might be associated with smoke. The equation for nonsoil K is:

$$KNON = (K - 0.6xFe). \quad (4-12)$$

Light-absorbing carbon (LAC): This is the total elemental carbon, determined as the sum of the two components ECLT and ECHT. These are included in the sum as determined, even if negative.

Soot by  $b_{abs}$ : Comparison with LAC gives an absorption efficiency of 20 m<sup>2</sup>/g, which is somewhat higher than that for diesel exhaust of 10 m<sup>2</sup>/g. For  $b_{abs}$  in 10<sup>-8</sup> m<sup>2</sup>, and an efficiency of 20 m<sup>2</sup>/g, the soot concentration in ng/m<sup>3</sup> is numerically equal to  $b_{abs}/2$ .

Organics by carbon (OMC): The total organic mass is the sum of the two measured organic concentrations (OCLT and OCHT). They are included in the sum as determined, even if negative. The total organic mass is obtained by multiplying the sum by 1.4 to include the noncarbon components of the organic particle. This assumes organics are 7% carbon.

Organics by hydrogen (OMH): The organic mass can also be calculated from the concentrations of hydrogen and sulfur measured on the Teflon filter. The measured hydrogen comes from organics, sulfate, nitrate, and water. It is assumed that all the sulfur is present as fully neutralized ammonium sulfate. It is also assumed that the nitrates and water volatilize from the filter during the exposure to a vacuum. These assumptions are invalid when there is high nitrate relative to sulfate, marine sulfur, or unneutralized sulfuric acid. The difference between the measured hydrogen and the hydrogen in sulfate is then organic hydrogen. The best fit between organic by carbon (OMC) and the organic hydrogen for most sites in the western United States, including all in the Washington area, is obtained by multiplying the organic hydrogen by 13.75. The organic carbon measurements indicate that 20% of the total organic mass is in the volatile fraction, volatilizing below 120°C. If it is assumed that 20% of the organic hydrogen also volatilizes in a vacuum, then the fit indicates that hydrogen accounts for 9% of the average organic particle. If it is assumed that no organic hydrogen is volatilized, the factor decreases to 7%. The equation of OMH is:

$$OMH = 13.75(H - 0.25xS). \quad (4-13)$$

If either H or S is invalid or not detected (below mdl), then OMH is not calculated. OMH may be negative when the sulfate is large and not fully neutralized. In this case, the estimate is not a valid measure of organics.

Reconstructed mass from the Teflon filter (RCMA): The reconstructed mass is the sum of sulfate, soil, nonsulfate potassium, salt, elemental carbon, and organic carbon. The only

components not included are water and nitrate. The variable RCMA is based only on the Teflon filter, using  $b_{abs}$  for elemental carbon and OMH for organic carbon. The equation for RCMA is:

$$RCMA = 4.125xS + SOIL + 1.4xKNON + 2.5xNa + 0.5xb_{abs} + OMH . \quad (4-14)$$

For RCMA to be calculated, PIXE, PESA, and LIPM must all have valid analyses. The 1.4 factor with KNON ensures consistency with the soil estimate; it exactly compensates for the removal of nonsoil K from soil. The salt (NaCl) concentration is estimated solely from Na, because some of the chlorine is volatilized from the Teflon filter during collection. If S, Na, or  $b_{abs}$  are below the mdl, mdl/2 is used as both concentration and precision. KNON is used as calculated, even if negative. If OMH is negative, a value of zero is used in the sum and RCMA will always be positive.

Reconstructed mass using carbon (RCMC): The second variable, RCMC, uses the carbon components from the quartz filter and the other components from the Teflon filter. As in RCMA, the sum does not include water and nitrates. The equation for RCMC is:

$$RCMC = 4.125xS + SOIL + 1.4xKNON + 2.5xNa + LAC + OMC . \quad (4-15)$$

#### 4.4.2 Artifact Estimation

One field blank was included with every seven normal samples. In addition, every quartz filter was followed by a secondary filter to include the organic gas component of the artifact.

Gravimetric mass: The mass artifact was based on 361 field blanks. Three field blank values were discarded because the pre-masses were significantly larger than the post-masses. The mean and standard deviation were  $22.3 \pm 24.6 \mu\text{g}$ . This artifact was considerably larger and more variable than in the normal network. The probable reason is that the cassettes were not purchased far enough in advance to permit proper aging. Comparisons between fine gravimetric mass and reconstructed mass at both secondary and primary sites, to be discussed in Section 4.5, showed that the mass intercept was not statistically different than zero. This indicated no major bias in the artifact measurement.

PIXE/PESA/LIPM: Analysis of selected field blanks by PIXE/PESA and of all field blanks by LIPM indicated no statistically significant artifacts.

Carbon: Twenty-one field blanks and 91 secondary filters were analyzed by TOR. The means and standard deviations for the four temperature ranges are shown in Table 4-7. The difference between the means corresponds to the organic gas artifact. The only one of the four variables with a statistically significant difference (a difference greater than twice the standard error of the differences) was OCHT. Thus, the gas adsorption artifact was measured as high temperature organic. The artifact was based on the measurements of the secondary filters.

Table 4-7. Means and standard deviations of secondary quartz filters and quartz field blanks. The bottom row is the difference and standard error of the difference.

	OCLT	OCHT	ECLT	ECHT
Secondary	3.4 ± 2.8	11.5 ± 5.1	0.6 ± 0.6	1.3 ± 0.8
Field blank	2.6 ± 2.6	8.7 ± 2.9	0.4 ± 0.4	1.1 ± 0.8
Difference	0.8 ± 0.6	2.8 ± 0.8	0.1 ± 0.1	0.2 ± 0.2

An examination of the measured concentrations indicates that these artifacts are reasonable. Only 1% of the concentrations for total organic, OCHT, total elemental, and ECLT have negative values. Over half of the OCLT concentrations are negative. This may indicate that the volatile organic component is highly variable.

Ions on nylon: The means and standard deviations of the four ion variables for the field blanks are listed in Table 4-8. The resulting concentration of normal samples for sulfate and nitrate indicate a reasonable artifact estimate: the lowest 1% of concentrations are all near zero. Half of the chloride concentrations are zero, as are two thirds of the nitrite concentrations.

Table 4-8. Means and standard deviations of nylon field blanks for sulfate, nitrate, chloride and nitrite ions.

Sulfate	0.779 ± 0.150 µg
Nitrate	0.460 ± 0.132 µg
Chloride	1.482 ± 0.616 µg
Nitrite	0.881 ± 0.448 µg

SO<sub>2</sub>: The mean and standard deviation of sulfate on the impregnated field blanks were 6.5 ± 2.0 µg. One-quarter of the SO<sub>2</sub> concentrations were negative. However, the minimum SO<sub>2</sub> concentration was less than two standard deviations from zero. The artifact, therefore, appears to be reasonable.

#### 4.4.3 Precision Estimate

The precision in the concentrations includes the standard deviations of the field blanks or secondary filters, the volume precision, and the fractional analytical precision associated with calibration.

The volume precision of 3% used in the IMPROVE network data was retained. In addition, the analytical precisions used in the IMPROVE network have been retained. These are

2% for saltation; 3% for nitrate; 4% for PIXE, PESA, OCLT and OCHT, and SO<sub>2</sub>; and 9% for ECLT and ECHT. The PREVENT replicate data indicated no significant variations from normal.

The average precision for each variable is listed in Table 4-9. Because of the compensating area of sample collection on the 12-hour samples, the PIXE/PESA precision for the 12-hour samples was the same as for the 24-hour samples at the secondary sites. This was not true for gravimetric mass; the precision for the 12-hour samples was clearly worse than for the 24-hour samples. TSO<sub>4</sub> and TNO<sub>3</sub> refer to measurements on the undenedud module.

Table 4-10 compares the precision for the various X ray analyses of the Tahoma Woods samples.

Table 4-9. Mean concentrations and precision of the mean value.

PIXE/PESA/LIPM on Teflon (primary and secondary)					
H	384	5.2%	Fe	38	5.2%
S	521	5.1%	Na	83	9.5%
Si	97	5.8%	V	1.5	23.1%
K	71	5.4%	Ni	1.0	13.7%
Ca	23	7.2%	Cu	1.3	11.1%
Ti	4.8	10.6%	Zn	4.9	6.1%
Mn	2.3	13.2%	As	0.7	25.5%
fine mass (primary)		8752	18.0%		
fine mass (secondary)		7938	9.8%		
PM <sub>10</sub> mass (primary)		17947	11.5%		
ion on nylon (primary)					
NO <sub>3</sub> <sup>-</sup>	240	6.0%	TNO <sub>3</sub>	296	5.5%
SO <sub>4</sub> <sup>=</sup>	1465	3.7%	TSO <sub>4</sub>	1473	3.7%
carbon on quartz (primary)					
OCLT	37	475.5%	ECLT	279	18.6%
OCHT	1906	18.1%	ECHT	202	28.2%
OC <sub>tot</sub>	1943	19.9%	EC <sub>tot</sub>	481	16.2%
SO <sub>2</sub> (primary)	588	20.4%			

Table 4-10. Mean calculated precision as percent of mean concentration for various analytical methods at Tahoma Woods.

Element	12-HR PIXE	24-HR PIXE	12-HR XRF	24-HR XRF	12-HR SRXRF	24-HR SRXRF
H	5.2%	5.4%				
Na	16.1%	18.5%				
Si	6.5%	5.7%				
S	5.1%	5.1%				
K	5.4%	5.3%				
Ca	8.3%	7.3%				
Ti	15.9%	11.0%				
Mn	13.4%	12.1%	7.7%	6.2%	6.4%	5.7%
Fe	5.4%	5.2%	5.2%	5.1%	5.1%	5.1%
V	42.2%	32.6%	17.4%	12.6%	13.7%	12.6%
Ni	67.1%	59.9%	12.9%	8.8%	8.4%	6.6%
Cu	18.8%	12.9%	7.4%	6.4%	6.3%	5.8%
Zn	5.9%	5.6%	5.3%	5.2%	5.1%	5.1%
As	36.1%	52.0%	5.8%	5.3%	17.1%	18.1%
Se	85.7%	57.8%	16.3%	10.3%	11.1%	7.6%
Br	11.4%	9.4%	7.4%	7.4%	5.4%	5.2%
Pb	13.6%	8.1%			5.4%	5.6%

## 4.5 DATA VALIDATION

This section summarizes the intercomparisons made in the data set. These are gravimetric mass and reconstructed mass, sulfur by PIXE and sulfate ion, organic by carbon and organic by hydrogen, light-absorbing carbon and the coefficient of absorption. In addition, intercomparisons between PIXE and XRF are included.

### 4.5.1 Gravimetric and Reconstructed Mass

Figure 4-1 compares gravimetric mass and reconstructed mass on the Teflon filter (RCMA) at all secondary sites and at all primary sites. The zero intercepts indicate a correct estimate of gravimetric artifact, as noted in Section 4.4.2. At the secondary sites, the reconstructed mass accounts for 92% of the gravimetric mass. The remainder is presumed to be water and nitrate. For all sites in the western United States for July and August 1988 and 1989, the reconstructed mass was 82% of the fine mass. However, for these same western sites, the

ratio dropped to 60%. Thus the remainder for the secondary sites is less than expected. At the primary sites, only 63% of the gravimetric mass is accounted for by the reconstructed mass. This is approximately the same as for all western sites for 1990. The larger scatter for the 12-hour data is associated with the gravimetric precision, which is twice that of the 24-hour data (18% vs 10%).

The comparison for the 12-hour samples using the reconstructed mass including the quartz measurements (RCMC) at the primary sites gave similar results to the 12-hour RCMA plot.

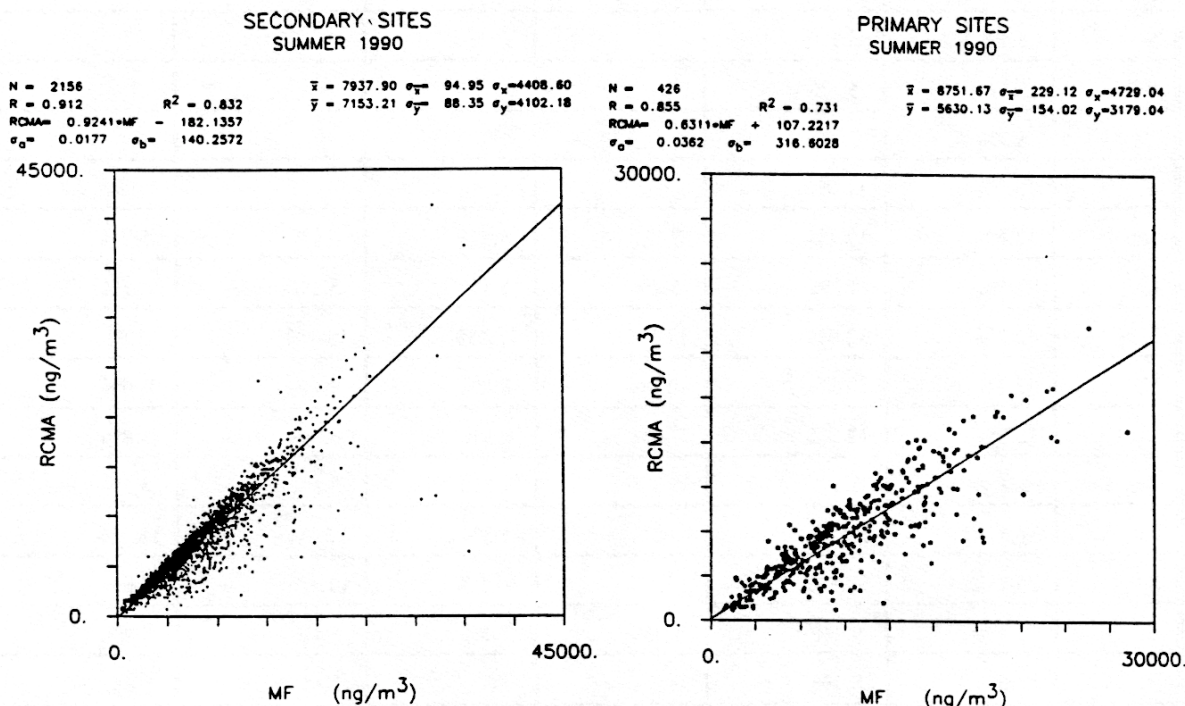


Figure 4-1. Comparison of fine gravimetric mass (MF) and reconstructed mass using hydrogen and absorption (RCMA) at the secondary sites. The line minimizes the perpendicular deviations. A diagonal line would indicate equality.

#### 4.5.2 Sulfate

Figure 4-2 time plots compare the three sulfate measurements at Tahoma Woods: sulfur on Teflon by PIXE times 3; sulfate on nylon with denuder by IC; and sulfate on nylon without denuder by IC. The three bivariate correlation coefficients ( $r^2$ ) are from 0.98 to 0.99.

#### 4.5.3 Organic Mass

Figure 4-3 compares organic by hydrogen with organic by carbon for the three primary sites. The left plot is for all points, and the right plot is with 30 points deleted. The OMH values were significantly higher than OMC for all data at Tahoma Woods and Marblemount after August 28. This accounted for 23 of the deleted points. A smaller effect was observed for this

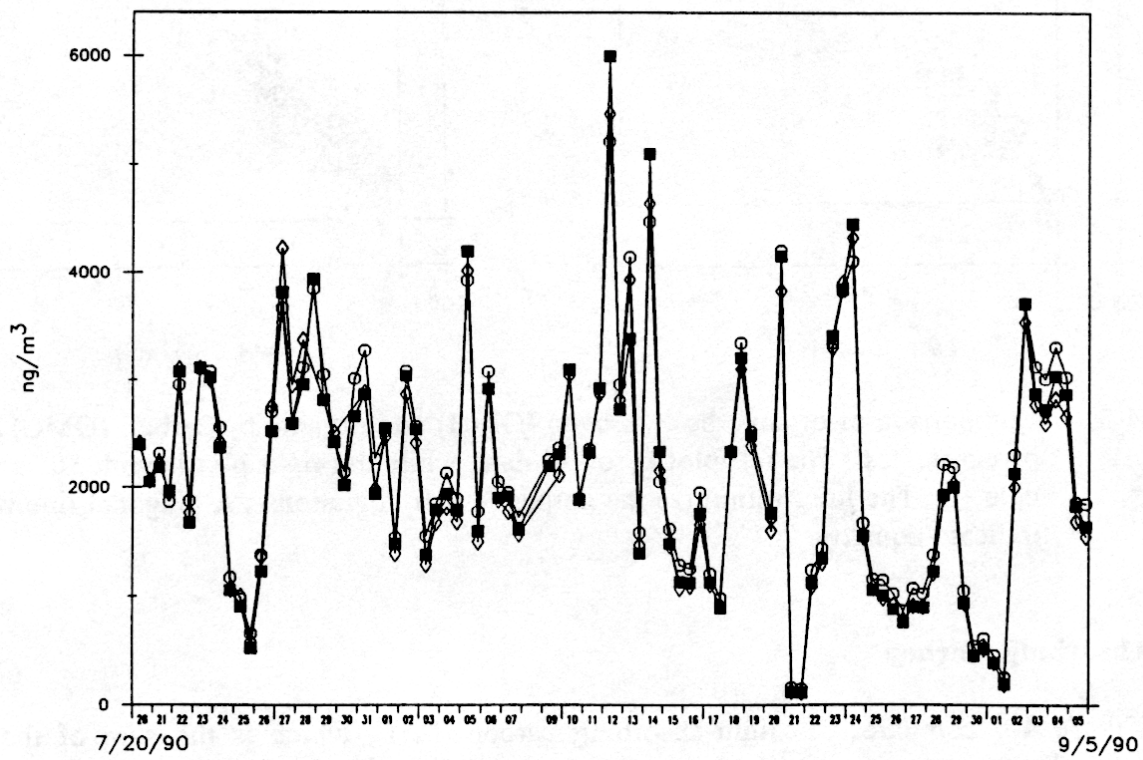
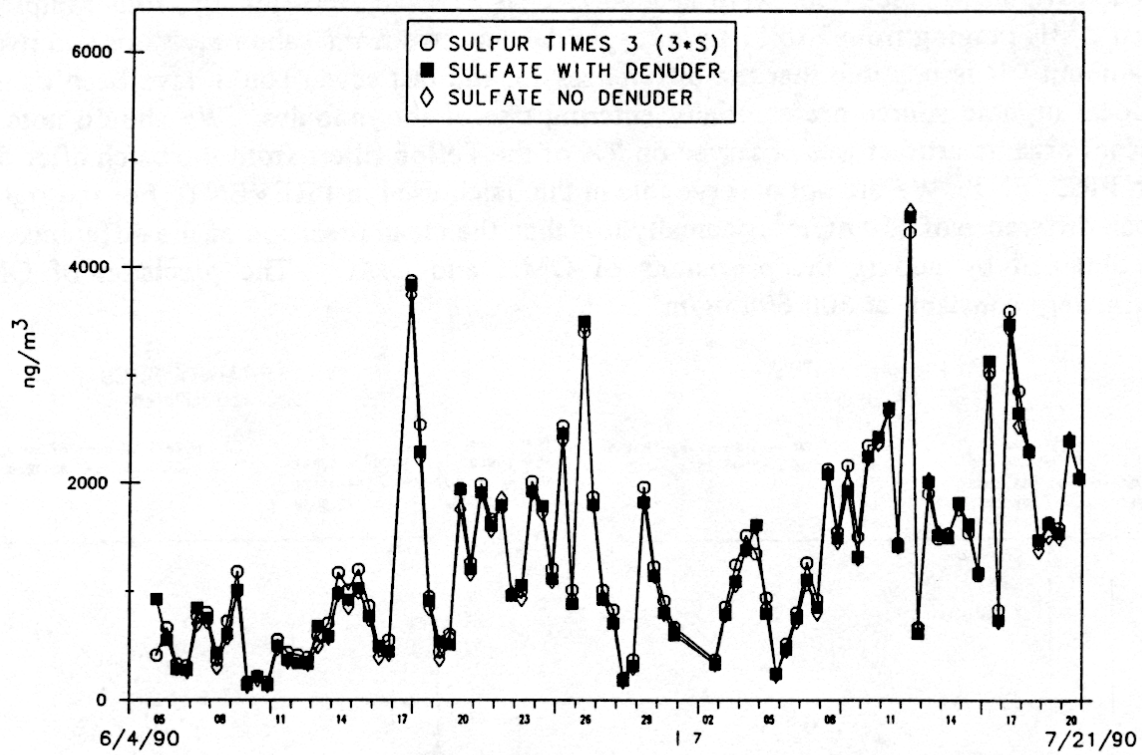


Figure 4-2. Time plots of all three sulfate measurements at Tahoma Woods.

period at Paradise, but the data was retained. In addition, three consecutive samples with elevated OMC at Marblemount were deleted (August 22 and 23). Finally, four samples with elevated OMH ranging from 3 to 11  $\mu\text{g}/\text{m}^3$  were deleted, two from Tahoma Woods and two from Marblemount. It is possible that the differences for the last seven could have been caused by some local organic source preferentially entering one of the modules. We should note that a significant organic artifact was observed on 7% of the Teflon filters from the batch after the one used in PREVENT. We did not observe this in the batch used in PREVENT. For the right plot, the mean difference of 550  $\text{ng}/\text{m}^3$  is actually less than the mean precision of the difference of 600  $\text{ng}/\text{m}^3$  obtained by adding the precisions of OMH and OMC. The precision of OMC is approximately constant, at 500-600  $\text{ng}/\text{m}^3$ .

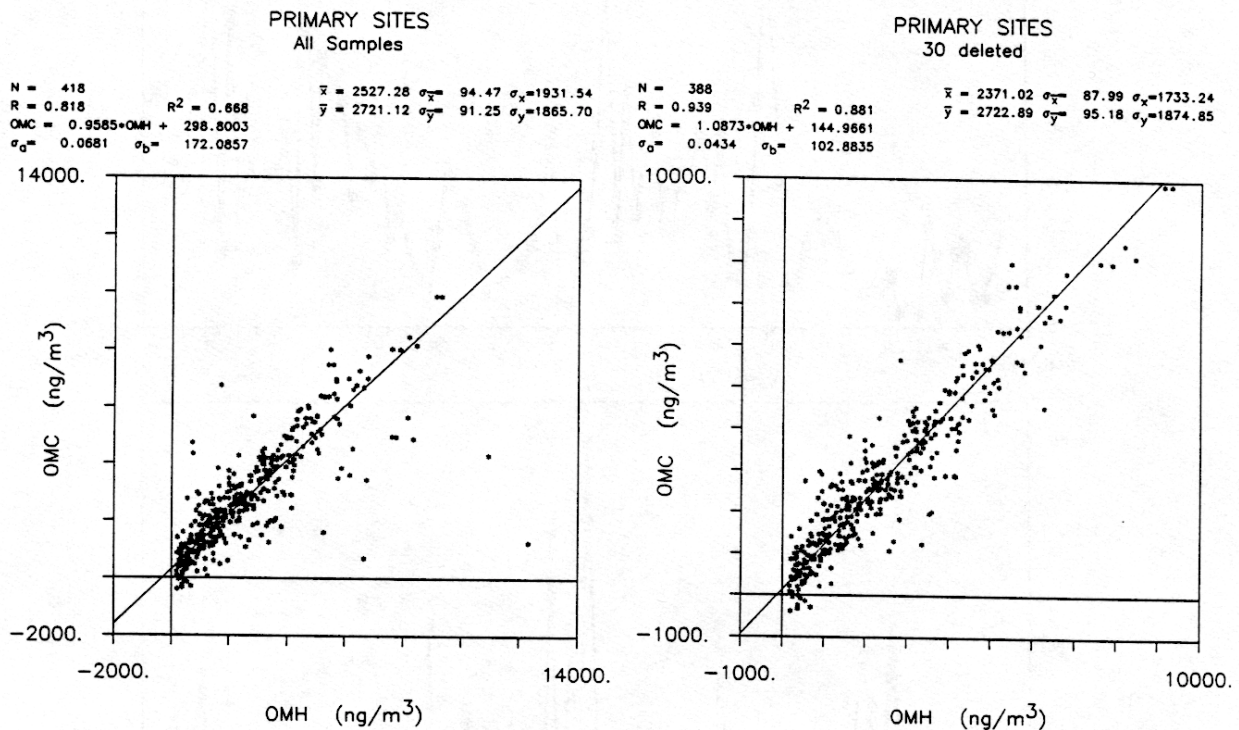


Figure 4-3. Comparison of organic by hydrogen (OMH) and organic by carbon (OMC) at all primary sites. The left plot is for all data, while the right plot is with 30 samples deleted. The lines minimize the perpendicular deviations. A diagonal line would indicate equality.

#### 4.5.4 Absorbing Carbon

Figure 4-4 compares the light-absorbing carbon, LAC, which is the sum of the two elemental carbon components measured on the quartz filter, with the coefficient of absorption measured on the Teflon filter. Tahoma Woods and Marblemount, the two lower sites, look quite similar and are combined into the left plot. The slope here is around 0.75. A slope of 1.0 is predicted for diesel soot, assuming that the LAC component includes all absorbing particles. One possibility is that some of the high temperature organic contributes to absorption. The higher elevation, Paradise site, shows less LAC relative to absorption.

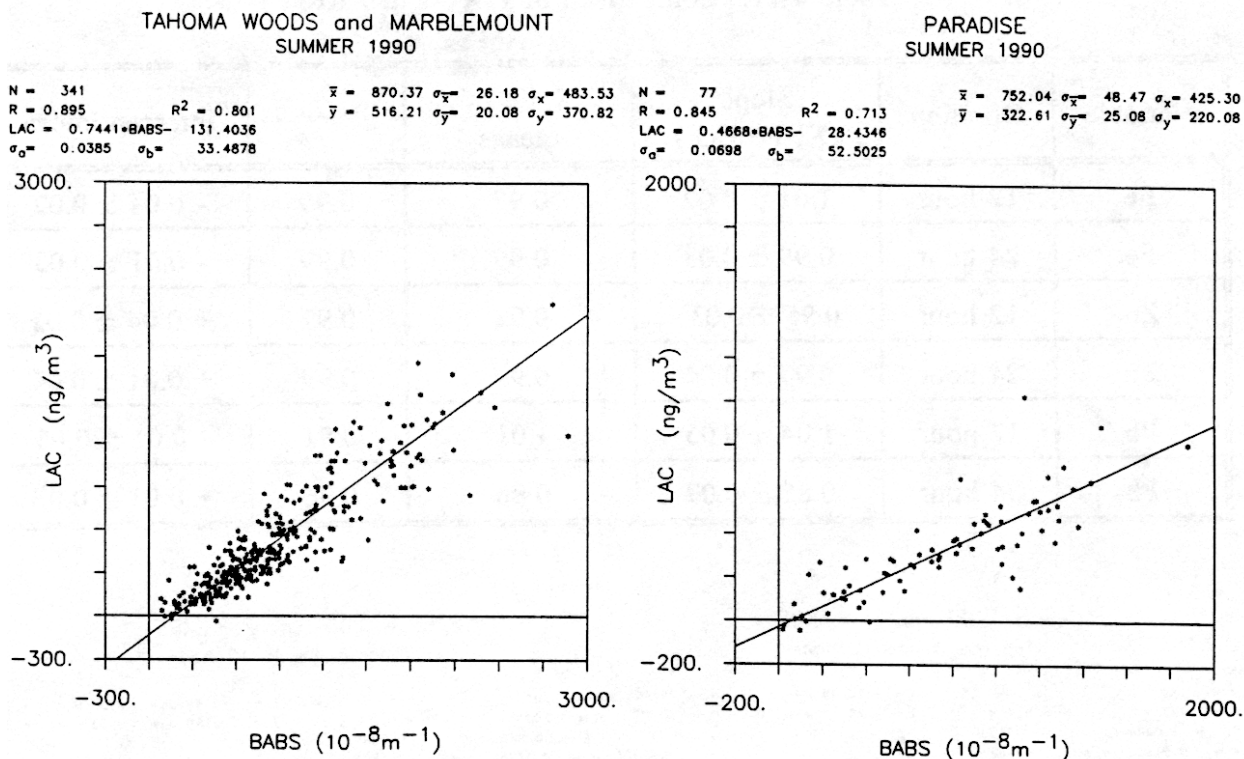


Figure 4-4. Comparison of light-absorbing carbon (LAC) and coefficient of absorption ( $b_{abs}$ ) in  $10^8 m^{-1}$ . The left plot is for Tahoma Woods and Marblemount, while the right plot is for Paradise. The lines minimize the perpendicular deviations. A diagonal line would indicate that LAC accounts for all absorption and has an absorption efficiency of  $10 m^2/g$ .

#### 4.5.5 PIXE and XRF

The UCD XRF system provides lower minimum detectable limits than the PIXE system for elements in the general region of Se. This section will deal with the question of how the two systems intercompared for elements that were measured above the mdl on nearly all samples, such as Fe, Zn, and Pb. Table 4-11 provides the important statistics for the comparisons between PIXE and XRF. The correlations are good, with  $r^2$  ranging from 0.91 to above 0.99. The slopes and ratios of means significantly differ from 1.0 in only one case. The intercepts do not significantly differ from zero. The conclusion is that the UCD PIXE and XRF systems gave equivalent results for these elements. Since the XRF precision is smaller than the PIXE precision, it is preferred for elements heavier than Fe. Figure 4-5 shows the comparison for the 12-hour Fe and Zn measurements at Tahoma Woods.

Table 4-11. Comparison of PIXE and XRF.

Variable	Duration	Slope (XRF/PIXE)	Ratio of means	$r^2$	Intercept/mean
Fe	12 hour	1.01 ± 0.02	0.97	0.99	- 0.04 ± 0.02
Fe	24 hour	0.99 ± 0.03	0.99	0.99	- 0.01 ± 0.03
Zn	12 hour	0.95 ± 0.03`	0.98	0.97	+ 0.04 ± 0.03
Zn	24 hour	0.97 ± 0.04	0.99	0.99	+ 0.01 ± 0.04
Pb	12 hour	1.04 ± 0.05	1.01	0.91	- 0.01 ± 0.05
Pb	24 hour	0.85 ± 0.07	0.86	0.96	+ 0.01 ± 0.08

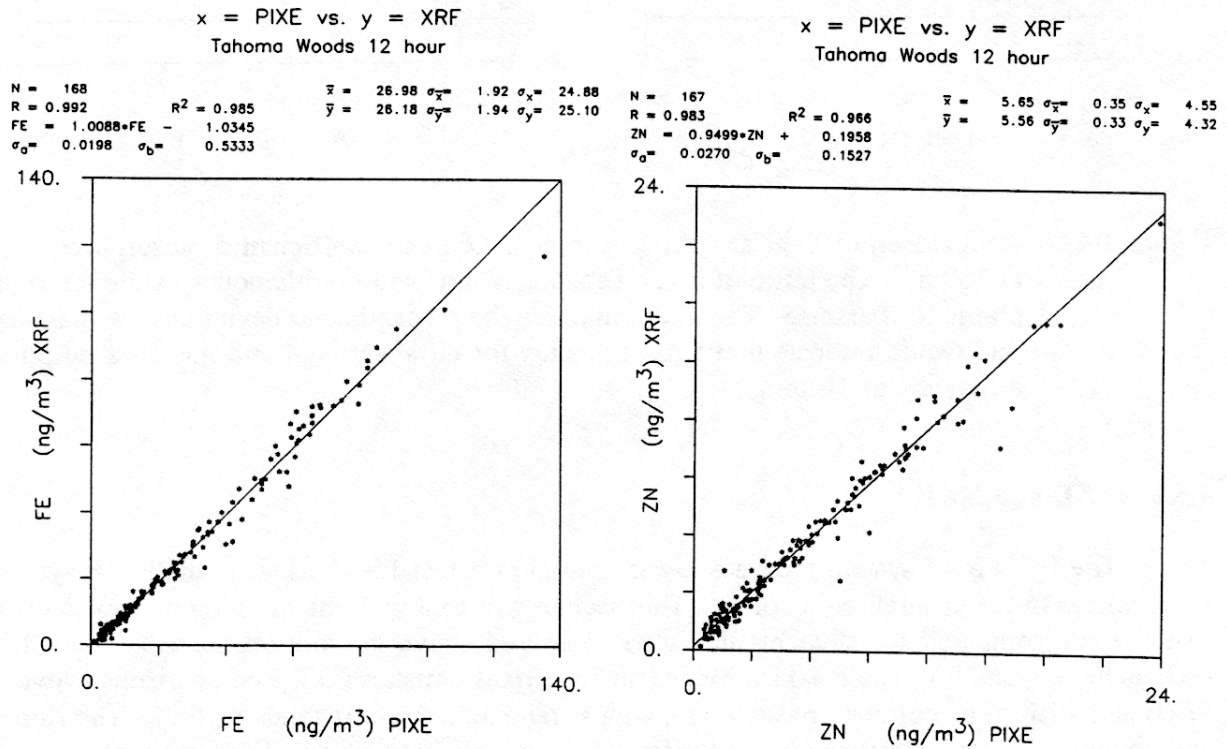


Figure 4-5. Comparison of PIXE and XRF for 12-hour measurements of Fe and Zn at Tahoma Woods. The lines minimize the perpendicular deviations. A diagonal line would indicate equality.

#### **4.6 AIRCRAFT RESULTS**

The results for the aircraft samples collected on July 25 and 26 are listed in Table 4-12. Gravimetric mass was omitted because the light loading did not permit reliable measurement. The calculation for soil differed slightly from Equation 4-11. Because Al could not be measured reliably with the light loadings, it was omitted from the soil calculation and the Si factor was increased from 2.42 to 3.01.

Table 4-12. Concentrations on aircraft samples.

Variable	Method	Centralia 7/25	Centralia 7/26	Urban 7/25	Burn 7/25	Burn 7/26	Bkgnd 7/25	Bkgnd 7/26	Units
Vol		1.39	1.40	0.95	0.75	0.48	2.82	2.41	m <sup>3</sup>
SO <sub>2</sub>	IC	12 ± 1	84 ± 7	69 ± 6	24 ± 4	5 ± 3	2 ± 1	1 ± 1	µg/m <sup>3</sup>
H	PESA	218	309	235	1295	1402	2082	6130	ng/m <sup>3</sup>
Si	PIXE	167	184	180	279	496	116	127	ng/m <sup>3</sup>
S	PIXE	349	345	338	372	809	350	202	ng/m <sup>3</sup>
Cl	PIXE	< 10	< 11	129	132	259	< 6	< 7	ng/m <sup>3</sup>
K	PIXE	28	38	79	470	329	30	27	ng/m <sup>3</sup>
Ca	PIXE	20	30	45	208	142	24	17	ng/m <sup>3</sup>
Ti	PIXE	6	10	31	10	< 17	6	18	ng/m <sup>3</sup>
V	PIXE	< 4	< 5	< 8	< 8	10*	5	5	ng/m <sup>3</sup>
Mn	PIXE	< 4	< 4	11	9	< 13	< 2	6	ng/m <sup>3</sup>
Fe	PIXE	23	35	35	58	66	24	37	ng/m <sup>3</sup>
Fe	XRF	23.5	40	2.2**	63	79	25	28	ng/m <sup>3</sup>
Ni	XRF	< 0.36	< 0.36	< 1.0	< 0.7	< 1.1	< 0.24	< 0.18	ng/m <sup>3</sup>
Cu	XRF	< 0.37	< 0.37	1.82**	4.13	< 1.1	0.22	0.87	ng/m <sup>3</sup>
Zn	XRF	2.50	1.53	2.89**	18.2	14.8	2.61	2.59	ng/m <sup>3</sup>
Pb	XRF	1.60	2.13	1.64**	6.25	7.60	1.50	0.98	ng/m <sup>3</sup>
Se	XRF	0.62±.17	0.67±.10	0.17	0.37	0.52	0.10	0.10	ng/m <sup>3</sup>
Br	XRF	0.84	0.79	0.76**	2.92	5.22	0.74	0.78	ng/m <sup>3</sup>
Rb	XRF	< 0.50	0.67	1.71**	3.16	1.89	< 0.27	< 0.25	ng/m <sup>3</sup>
Sr	XRF	2.15	1.95	< 0.7	4.90	4.67	2.13	0.50	ng/m <sup>3</sup>
b <sub>abs</sub>	LIPM	6.2	6.6	3.4	23.7	33.6	4.6	2.0	10 <sup>-6</sup> m <sup>-1</sup>
RCMA		4.2	5.6	4.6	21.4	24.1	29.6	85.1	µg/m <sup>3</sup>
OMH		43	55	45	77	68	93	98	%
NHSO		35	26	30	7	14	5	1	%
soil,K,Cl		15	13	21	10	11	2	1	%
soot		7	6	4	6	7	1	0	%

\*\* The urban plume sample was torn after the PIXE analysis and before the XRF analysis.

## REFERENCES

1. Eldred, Robert, 1989. Standard operating procedures for IMPROVE particulate monitoring network. Analytical Division, Crocker Nuclear Laboratory, University of California, Davis. July.